JOURNAL OF MATERIALS SCIENCE 25 (1990) 3380–3384

Crystallization of carbon fibre reinforced polypropylene

JOÃO K. TAN*, TAKESHI KITANO‡, TATSUKO HATAKEYAMA‡
*Centro de Pesquisa e Desenvolvimento, Km O da Rod. Ba. 512, Cx. Postal 09, CEP- 42800, Camacari, Bahia, Brazil
‡Research Institute for Polymers and Textiles, 1-1-4, Higashi, Tsukuba, Ibaraki 305, Japan

Polypropylene (PP) was compounded with carbon fibre of various contents (0, 5, 10, 15, 20 vol %) using a single and a twin screw extruder. The influence of both the carbon fibre content and the compounding method on the thermal behaviour and characteristics of crystallization was studied using differential scanning calorimetry (DSC), polarizing optical microscopy and scanning electron microscopy (SEM). Melting and crystallization temperatures increased with the amount of carbon fibre. Isothermal crystallization was observed using DSC and it was found that crystallization was accelerated by the presence of carbon fibres. Using polarizing optical microscopy, it was found that the nucleation of polypropylene started at the crossing point of two or more fibres.

1. Introduction

Polypropylene (PP) is representative of semicrystalline polymers and is widely used in various fields in view of its versatility in many types of processing techniques. The higher order structure of this type of polymer depends on the cooling conditions from the molten state, especially the cooling velocity inside the mould of any moulding process. The cooling condition affects spherulite size and the degree of crystallinity and in consequence also the physical and mechanical properties.

Many high performance semicrystalline thermoplastic composites have already been commercially used in the production of motorcars and aeroplanes. The physical and mechanical properties of semicrystalline polymers reinforced with glass fibre [1–3], carbon fibre [4, 5] and other types of fillers [6] have been previously cited. Glass fibre was added to PP and polyethylene and the effect on the crystallization behaviour has been studied by thermal analysis [3, 7]. Inorganic filler with different surface characteristics and also the influence of interfacial force has been studied [8]. The influence of the interface on the crystallization of PP has also been reported [8–10]. The rheological properties of fibre and inorganic filler reinforced polymers have been investigated in detail [11–15].

In spite of the extensive application of PP composites, few papers have been published on the crystallization mechanism of PP reinforced with fibres or fillers. The aim of this paper is to study the influence of carbon fibre on the crystallization mechanism and the thermal properties of fibre-reinforced PP using differential scanning calorimetry (DSC).

2. Experimental procedure

2.1. Materials

The isostatic PP used in this study was supplied by Sumitomo Co. with code Noblen W 101 (zero shear viscosity $\eta_0 = 5.5 \times 10^3$ Pa sec). Carbon fibre free from any surface treatment was supplied by Toho Rayon Co.

2.2. Sample preparation

The following two methods were used for mixing the fibres with PP.

2.2.1. Compounding with a single screw extruder

Weighed amounts of PP and fibres (chopped strand) were inserted in an extruder (Brabender-OHG/Plasticorder PLV 151 – Duisburg, diameter $D = 19$ mm, $L/D = 20$) which was operated at 220° C with a screw rotation of 25 r.p.m. The extruded samples were cooled in a water bath and cut into pellets of about 5 mm in length by a pelletizer. After drying in an air oven, the pellets were extruded twice in order to obtain well dispersed samples [11]. The obtained samples were designated in the following way; PP1 for pure PP, CF5-1, CF10-1, CF15-1 and CF20-1 for the samples with carbon fibres content of 5, 10, 15 and 20 vol %.

2.2.2. Compounding with a twin screw extruder

Weighed amounts of PP and fibres were inserted in a twin extruder (Tsukada Juki Co. Ltd. – Japan/RT35-2S, diameter 35 mm, $L/D = 15$) at 220° C. The obtained samples were designated in the following way; PP2 for pure PP, CF5-2, CF10-2, CF15-2 and CF20-2 for samples with carbon fibres content of 5, 10, 15, 20 vol %.

2.2.3. Preparation of the testing samples

The pellets prepared by each of the above methods were press-moulded (180° C, 5 atm.) into a 3 mm thick

0022–2461/90 $03.00 + .12

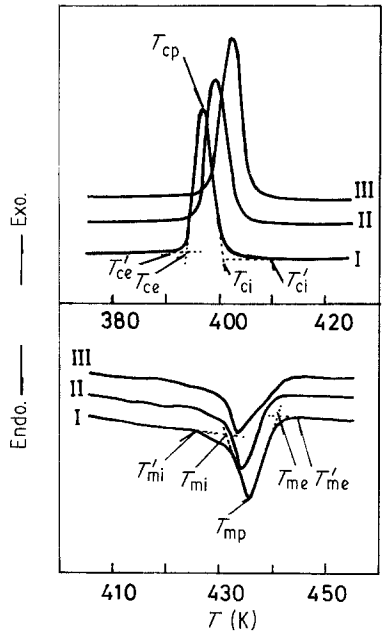

Figure 1 DSC melting and crystallization curves of original PP (I), single screw extruded PP (II) and twin screw extruded PP (III).

sheet. Samples for thermal characterization testing were cut from this sheet.

2.2.4. Fibre contents and the distribution of the fibre length in the samples

The fibre content (weight fraction) was determined [11] gravimetrically after incinerating the matrix material. The volume fraction of the fibre was determined at 23° C. To examine the fibre length distribution, the incineration residue was immersed in water and each filament dispersed separately. After some agitation of the fibre dispersion, it was spread on a glass plate and after removing the water the overall feature was photomicrographed. From this photograph the length of each filament was measured and the distribution of the lengths in the testing samples was determined.

3. Measurements

3.1. Differential scanning calorimetry

A Perkin Elmer DSC-2 was used for measuring the melting and crystallization temperatures and the characteristics of isothermal crystallization of PP composite. The sample weight was about 4 mg, the heating rate 10 K min^{-1} and the temperature range between 320 and 480 K. In order to eliminate the thermal history, the sample was heated to 480 K and maintained at that temperature for 5 min. The transition temperatures were defined as shown in Fig. 1.

The technique used to obtain the isothermal crystallization curve was the same as that described by Kamide [16]. In order to minimize any influence of previous thermal history, the sample was held in the molten state at about 30 K above the melting temperature (480 K) for 5 min. The sample was quickly cooled to crystallization temperature and the exothermic curve was recorded as a function of time. The isothermal temperature starting point was defined when the power was supplied to the sample holder.

3.2. Optical polarizing microscope

A Leitz polarized light microscope (Orthpolan Pol) equipped with heating stage and camera was used to observe the crystal nucleation.

3.3. Scanning electron microscopy

A Hitachi scanning electron microscope (S-500A) was used for observation of the fracture surface of PP composite.

4. Results and discussion

Fig. 1 shows the DSC melting and crystallization curves of PP samples without carbon fibre prepared as described in the experimental section. The first heating run was not included in this figure, because the DSC curves were affected by their thermal and mechanical histories during the sample preparation. Curve I represents original PP pellets, curve II PP processed in the single screw extruder (PP-1) and curve III the curve of PP processed in the twin screw extruder (PP-2).

A comparison of these three curves shows that the processing condition had a marked influence on the melting and crystallization curves. For example, the peak temperature of crystallization shifted to the lower temperature 391, 388 and 386 K for PP, PP-1 and PP-2, respectively. The shifting of the peak temperature of melting and crystallization to the low temperature side is attributed to decrease in molecular weight caused by mixing in the extruder. As reported in our previous paper, zero shear viscosity of PP-1 (η_{10}) was 5.55×10^3 Pa sec and that of PP-2 (η_{20}) was 3.05×10^3 Pa sec. If we assume the equation $\eta_0 \propto$

TABLE I Sample specifications

Code	Volume fraction of fibres at 23° C (%)	Number average length, l_N (mm)	Compounding method
PP-1	0	–	
CF5-1	5	0.447	Single screw
CF10-1	10	0.387	extruder
CF15-1	15	0.292	
CF20-1	20	0.286	
PP-2	0	–	
CF5-2	5	0.334	
CF10-2	10	0.325	Twin screw
CF15-2	15	0.273	extruder
CF20-2	20	0.225	

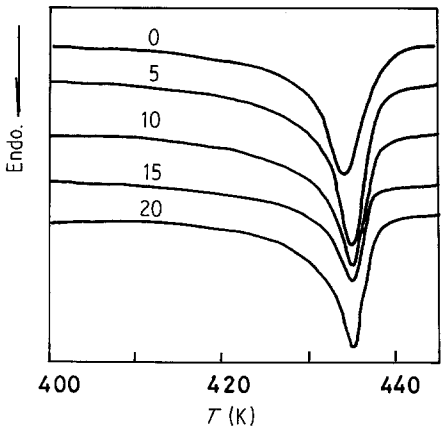

Figure 2 DSC melting curves of PP reinforced with carbon fibre. Numerals in the figure show fibre content: 0, PP1; 5, CF5-1; 10, CF10-1; 15, CF15-1; 20, CF20-1.

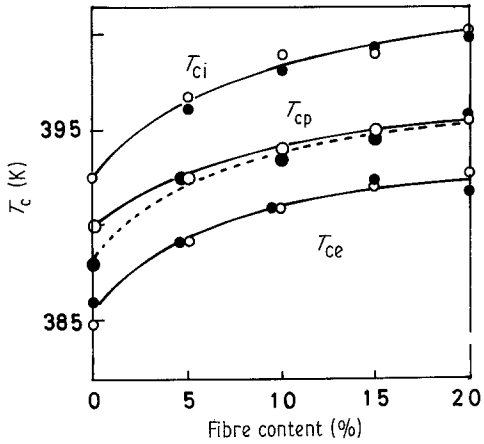

Figure 4 Relationship between crystallization temperature of PP and carbon fibre content. T_{ci} is the extrapolated onset temperature, T_{cp} the crystallization peak temperature and T_{ce} the extrapolated end temperature. (○ CF-1, ● CF-2).

$M^{3.4}$ is applicable to the sample, $M_{PP1} \approx 1.2\, M_{PP2}$ can be obtained, where M_{PP1} and M_{PP2} are weight average molecular weights. This suggested that thermal degradation of PP took place during moulding. At the same time, it is considered that the shear stress which occurred in the twin extruder also accelerated the degradation of PP.

Table I lists the samples for both compounding methods and the average length of carbon fibre (l_N) in each sample after moulding. As it can be seen, the compounding method affects not only the polymer stability but also the length of the carbon fibre. The fibres were severely broken by the intense mixing method. The average length of the fibres in the samples prepared in the twin screw extruder was smaller than that prepared in the single screw extruder. This is probably due to friction between the fibres during the compounding. The average length of carbon fibres became smaller with increasing amount of carbon fibre. The samples prepared using the single screw extruder showed longer average length of fibre than those prepared using the twin screw extruder.

Figs 2 and 3 show DSC heating and cooling curves of fibre reinforced PP. It can be clearly seen that the crystallization peak shifted to the low temperature side with increasing fibre content, and the melting peak was broadened by adding carbon fibre, although the melting temperature range did not show any variation.

The influence of fibre content on the crystallization and melting temperatures is shown in Figs 4 and 5. In these figures, it is possible to observe that the crystallization peak temperature (T_{mp}) of the sample with 5% carbon fibres increased by 4 and 8 K for single and twin screw extruders, respectively. This tendency to increase was observed in both series of samples as the carbon fibre amount increased to 20%. Although T_{mp} did not show any variation with increasing amount of carbon fibre, the melting temperature range became narrower with addition of carbon fibre.

Fig. 6 shows the isothermal crystallization curves at 398 K of PP (Fig. 6a), CF-PP-1 (Fig. 6b) and CF-PP-2 (Fig. 6c). It is clearly seen in Fig. 6a that the time interval of crystallization increased with intense mixing, suggesting a decrease in molecular weight. At the same time, the exothermic peak (t_{max}) of both series of carbon fibre reinforced PP decreased with increasing fibre content as shown in Figs 6b and 6c. These isothermal crystallization curves indicated that carbon fibre accelerated the crystallization rate in both series of samples.

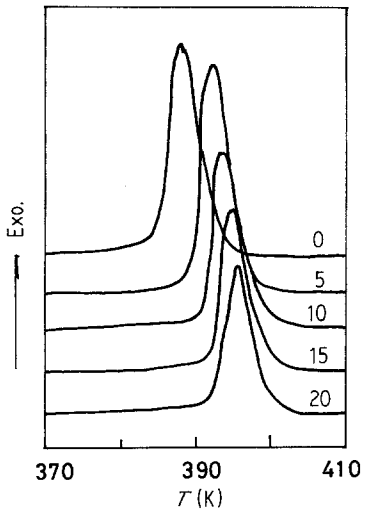

Figure 3 DSC crystallization curves of PP reinforced with carbon fibre. Numerals in the figure shows fibre content. 0, PP1; 5, CF5-1; 10, CF10-1; 15, CF15-1; 20, CF20-1.

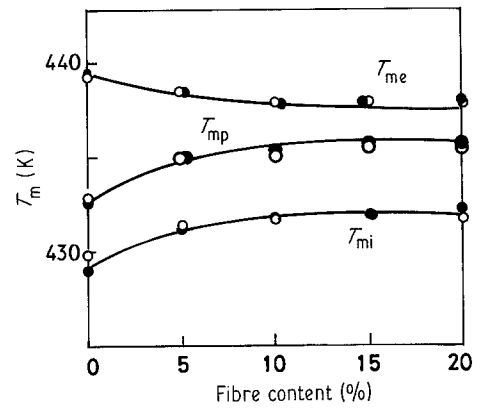

Figure 5 Relationship between melting temperature and carbon fibre content. T_{mi} is the extrapolated onset temperature, T_{mp} the melting peak temperature and T_{me} the extrapolated end temperature. (○ CF-1, ● CF-2).

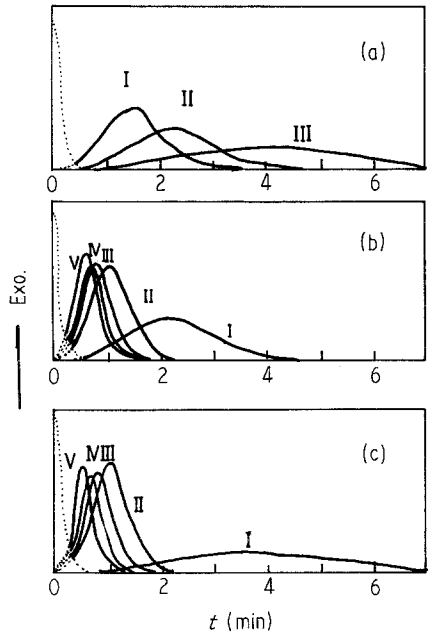

Figure 6 Isothermal crystallization curve of PP (a) I, PP pellets, II, PP processed in single screw extruder; III, PP processed in twin screw extruder. (b) I, PP1; II, CF5-1; III, CF10-1; IV, CF15-1; V, CF20-1. (c) I, PP2; II CF5-1; III, CF10-2; IV, CF15-2; V, CF20-2.

The isothermal crystallization curves shown in Fig. 6 were applied to Avrami's equation, $\ln X = -kt^n$ [17]. In this equation, X is the fraction of material which has not yet transformed at time t, and k and n are constants. X can be represented by the ratio $(\Sigma H - \Sigma H_t)/\Sigma H (\equiv \theta)$, where ΣH is the total area of observed exothermic peak and ΣH_t is the area of observed exothermic peak from the starting of crystallization to t_{min}.

The relationships between ln (ln θ) and t of single screw extruded PP with various fibre contents are shown in Fig. 7. Indices (n) obtained from the slope of Avrami's plot were around 3. This suggests that crystals grow three-dimensionally and carbon fibres accelerate the crystallization time without changing the type of crystal nucleation.

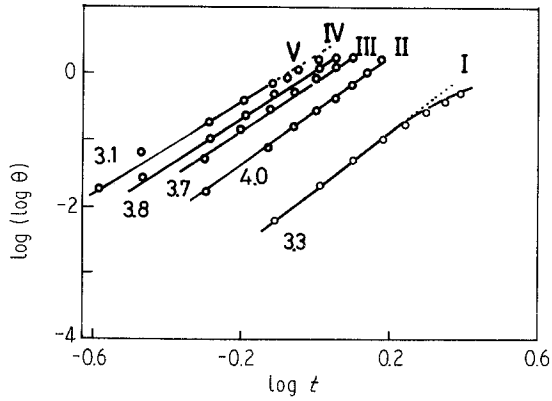

Figure 7 Avrami plot at 398 K of PP reinforced with carbon fibre prepared by a single screw extruder: I, PP1; II, CF5-1; III, CF10-1; IV, CF15-1; V, CF20-1.

Table II shows the variation of Avrami's index n for the samples of PP with and without carbon fibre. The calculated n values were about 3, although the compounding methods or crystallization temperature were varied.

Fig. 8 shows the polarizing micrographs of the nucleation of crystals at 400 K. As seen from Fig. 8 the presence of carbon fibres in the polymer matrix neither acts as a nucleation agent nor disturbs the nucleation around the fibre. Fig. 8a shows that nucleation starts preferentially at the crossing point of two or more fibres. Fig. 8b shows the crystal of CF5-2. The spherulite are smaller than those obtained from the pure PP. This photo suggests that carbon fibres restrict the molecular transportation of crystal growth. Fig. 8d suggests that the presence of a large number of fibre crossing points decreases the size of crystals.

Fig. 9 shows the electron scanning micrographs of

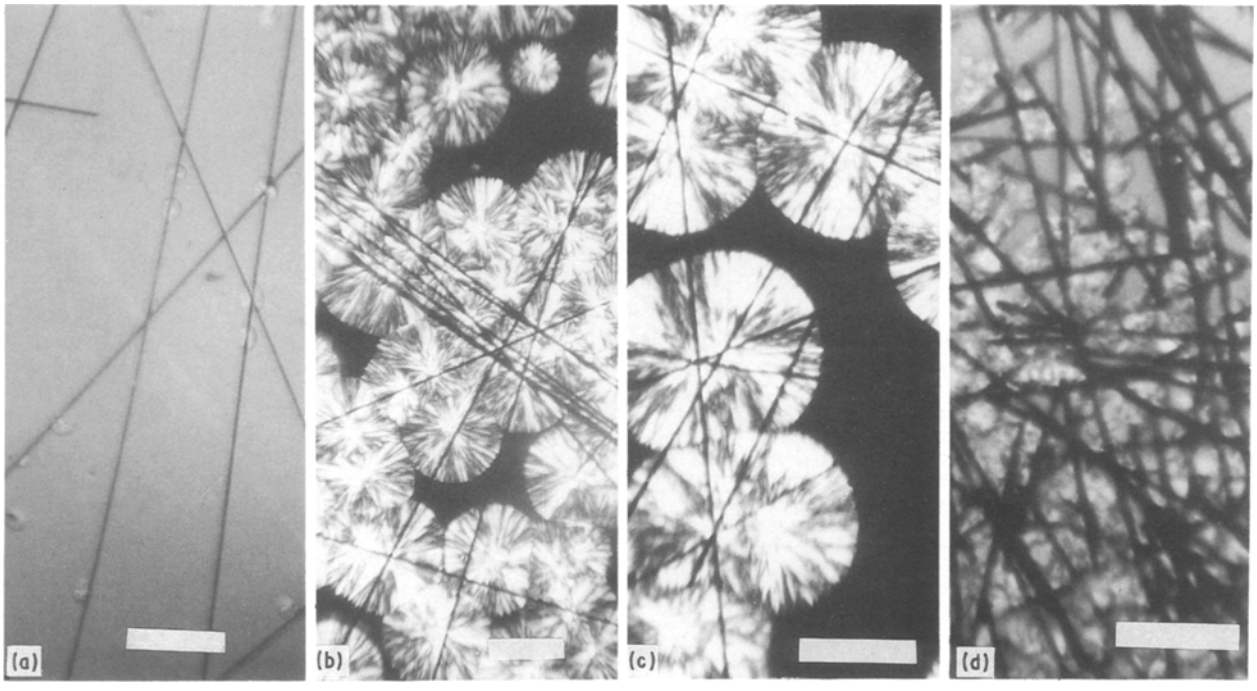

Figure 8 Polarizing light micrographs of PP reinforced with carbon fibres. (a) scale bar = 200 μm. (b)–(d) scale bar = 100 μm.

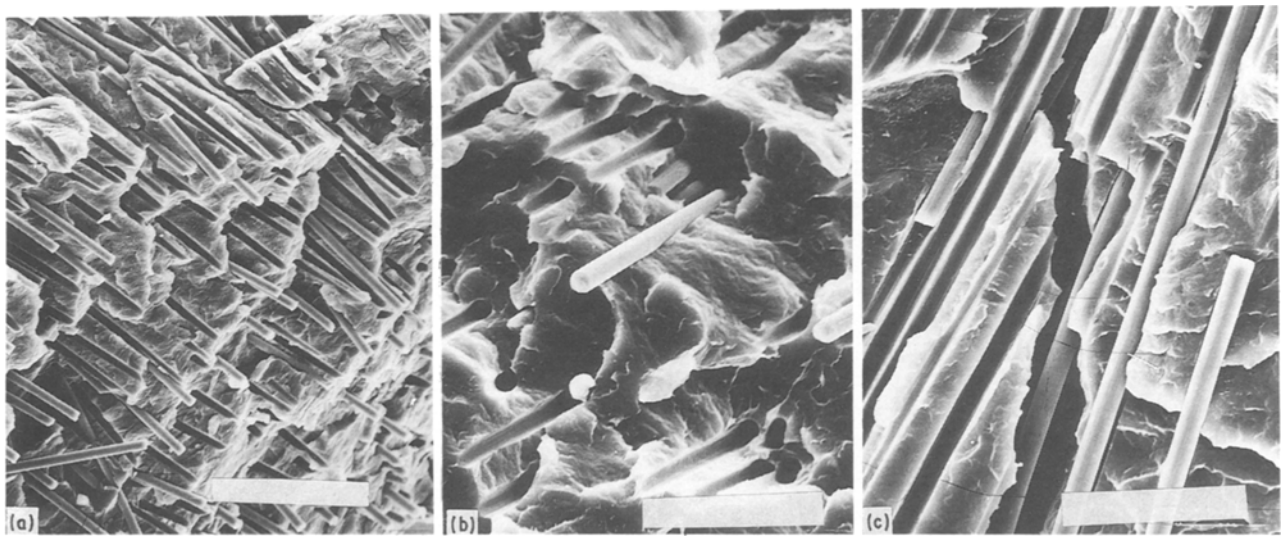

Figure 9 Scanning electron micrographs of PP reinforced with carbon fibres. (a) scale bar = 100 μm, (b), (c) scale bar = 50 μm.

fracture surface of CF5-2. Fig. 9a indicates that carbon fibres are easily released from the polymer matrix suggesting that the sample was fractured without adhesive force. Fig. 9b is an enlarged picture showing holes where long fibres were extruded. Fig. 9c shows the interface between carbon fibre and PP. It is clearly seen that carbon fibres were separated from the matrix.

5. Conclusion

From the results of thermal analysis, it was suggested that the compounding methods strongly affected the crystallization behaviour of PP, i.e. the crystallization peak shifted to the low temperature side and the isothermal cyrstallization time increased with intense mixing. At the same time, the length of mixed carbon fibre decreased with increasing fibre content. These facts indicated that the molecular weight of PP decreased as a result of thermal and mechanical degradation. Intrinsic viscosity data agreed well with the above result. It was also found that the crystallization of PP was accelerated in the presence of carbon fibres, although the crystallization mechanism did not change. Avrami's indices calculated from isothermal crystallization curves of PP samples with and without carbon fibres were almost the same. This indicates that the crystallization occurred three dimensionally in PP even if carbon fibre was added. At the same time, DSC data showed that the crystallization was accelerated when carbon fibre was present in PP. This suggests that crystal growth is affected by the compatarimerization and the distance of molecular transportation is shortened by the carbon fibre. Polarizing microscopic study showed that the crystallite initially appeared near the crossing point of fibres and also that crystal growth was disturbed by carbon fibres. The size of spherulite grown in the PP matrix surrounded by carbon fibre is smaller than that found in PP without carbon fibre.

TABLE II Avrami's index, n of samples

Samples specifications	Index n	Samples specifications	Index n
PP-1	3.3	PP-2	2.4
CF5-1	4.0	CF5-2	3.8
CF10-1	3.7	CF10-2	3.5
CF15-1	3.8	CF15-2	3.3
CF20-1	3.1	CF20-2	3.1

T_c = 389 K.

References

1. A. F. XAVIER and A. MISRA, *Polym. Compos.* **2** (1985) 93.
2. A. K. GUPTA, V. B. GUPTA, R. H. PETERS, W. G. HARLAND and J. P. BERRY, *J. Appl. Polym. Sci.* **27** (1982) 4669.
3. D. M. BIGG, *ibid.* **1** (1985) 20.
4. K. J. NANGRANI and S. R. GERTEISEN, in Proceedings of the 42nd Annual Conference, Composite Institute Feb. 2–6, Session 5-B. (The Society of the Plastics Industry, Cincinnati, U.S.A., 1987).
5. J. M. CROSBY, K. TALLEY and T. R. DRYE, in Proceedings of the 42nd Annual Conference, Composite Institute, Feb 2-6, 1/Session 5-A. The Society of the Plastic Industry, Cincinnati, U.S.A., 1987).
6. D. L. FAULKNER, *J. Appl. Polym. Sci.* **36** (1988) 467.
7. T. HATAKEYAMA, T. KITANO and C. KLASON, *Int. Polym. Proc.* **4** (1988) 230.
8. V. A. KARGIN, T. I. SOGOLOVA, N. Ja. RAPOPORT and I. I. KURBANOVA, *J. Polym. Sci.* **16c** (1967) 1609.
9. F. L. BINSBERGEN, *Polymer* **11** (1970) 253.
10. D. R. FITCHMUN and S. NEWMAN, *J. Polym. Sci.* **8A** (1970) 1545.
11. T. KITANO, M. FUNABASHI, C. KLASON and J. KUBAT, *Int. Polym. Proc.* **III** (1988) 67.
12. T. KATAOKA, T. KITANO, M. SASAHARA and K. NISHIJIMA, *Rheol. Acta* **17** (1978) 149.
13. T. KITANO and T. KATAOKA, *ibid* **19** (1980) 753.
14. T. KITANO, T. KATAOKA and Y. NAGATSUKA, *ibid* **23** (1984) 408.
15. T. KITANO, T. KATAOKA and T. SHIROTA, *ibid.* **20** (1981) 207.
16. K. KAMIDE and K. FUJII, *Kobunshi Kogaku,* **24** (1967) 262.
17. M. AVRAMI, *J. Chem. Phys.* **7** (1939) 1103.

Received 6 April
and accepted 14 September 1989